Nonlinear Dirac Points and topological invariant in coupled hexagonal lattices

Fude Li[1], and X. X. Yi[1,2*]
[1] *Center for Quantum Sciences and School of Physics, Northeast Normal University, Changchun 130024, China*
[2] *Center for Advanced Optoelectronic Functional Materials Research, and Key Laboratory for UV Light-Emitting Materials and Technology of Ministry of Education, Northeast Normal University, Changchun 130024, China*
(Dated: October 18, 2021)

Topological phases and materials have attracted much attention in recent years. Though many progress has been made, the effect of nonlinearity on such system remains untouched. In this paper, by considering the mean-field approximation in a coupled boson-hexagonal lattice system, we obtain a different type of Dirac cone. Due to its special structure of the cone, the Berry phase(two-dimensional Zak phase) of this new Dirac cone is quantized differently, i.e., it has been modified due to the interactions and the critical line between different topological phases has moved, depending on the type of interactions. Furthermore, the new Berry phase is found to be quantized, offering a possible nonlinear topological invariant which can supply as a criterion of topological classification for that interacting system. The quantum phase transition in terms of this criterion in the system has also been examined.

PACS numbers:

I. INTRODUCTION

The geometric and topological ideas developed in the study of the band theory of solids has a far-reaching impact on modern condensed-matter physics[1–4]. Topological phase transitions have been of tremendous interest in recent condensed matter physics[5–8]. In lower dimensions, topological invariants are known to play a crucial role in classifying various phase transitions[9]. A typical example is the integer quantum Hall transition[10], where quantized Hall conductances are given by Chern numbers associated with the Berry connection[11] and its extension to the case of spin currents is also interesting. These topological invariants present a chance to characterize quantum materials.

Recently, topological phase in coupling systems have attracted much attention[12–15]. After the topological classification of noninteracting topological insulators, a general topological classification of interacting systems[16–18] becomes an interesting topic. Though developing the connection between topology and interaction requires advanced many-body techniques, which is often difficult, mean-field approaches may be still useful. Here, we take a mean-field approach to a interactional bosonic hexagonal lattice model, which is often used to study Bose-Einstein condensate[19, 20]. This leads to a nonlinear problem, and then the Bloch states are eigenstates of the Gross-Pitaevskii (GP) equation depicting a two-dimensional tight-binding hexagonal lattice with an on-site mean-field potential which is related to eigenstates. GP equations are a well-known tool to study the Bose-Einstein condensate of cold atoms gas. Moreover, GP equations are also useful in the study of photonic systems with Kerr nonlinearity.

As already learned from zero- or one-dimensional systems, the band structure arising from solving the stationary GP equation may produce self-crossing loop structures[21, 22]. This feature in two-dimensional situations suggests the loss of a well-defined Chern number as a topological invariant. In the vicinity of the self-crossing point of a 2D looped band, we discover the formation of a different type of 2D Dirac cone-Nonliear Dirac cone(NDC)[23].

As a remarkable finding detailed below, we will give a nonlinear Berry phase associated with adiabatic path in the reciprocal space enclosing a Nonlinear Dirac point by virtue of aidabatic theory. Hexagonal lattice model provides a stimulating example where the Berry phase can be a candidate for topological invariants in interactional systems. Due to mean-field method, we can make additional term in Berry phase with interactions.

This paper is organized as follows. In Sec. II, we derive a model Hamiltonian of interactional bosonic hexagonal lattice model which can be realized in photonic waveguide systems including the Kerr effect. The emerging Nonlinear cones and its effective Hamiltonian are also given for the model in this section. In Sec. III, we compute the Berry phase in nonlinear system and analyzed the Berry phase in effective Hamiltonian and state dependent Hamiltonian. And in Sec. IV, we give corresponding numerical results based on adiabatic evolution, then we conclude that Berry phase is associated with observable AB phase. In Sec. V, we consider some other situations for this model. In Sec. VI, we make some important discussion based proposed interactional bosonic hexagonal lattice model and we get the relationship among observable AB phase, interactional strength κ and on-site potential u. In Sec. VII, we summarize our results and make conclusions.

*yixx@nenu.edu.cn

II. INTERACTIONAL BOSONIC HEXAGONAL LATTICE MODEL

Recently, topological photonics[24] has been a rapidly emerging field of research in which geometrical and topological ideas are exploited to design and control the behavior of light and meanwhile recent advances have shown how to engineer photons. Thanks to the flexibility and diversity of photonics systems, this field provide new opportunities for realization of exotic topological models. Experimentally, it provide a wide range of platforms, including photonic crystals, waveguides, metamaterials, cavities, optomechanics, silicon photonics, and circuit QED, which can realize different topological phases.

For photonic systems with nonlinear optics, we will pay attention to the Kerr nonlinearities in terms of interaction between photons. The standard semiclassical description of nonlinear optical processes is based on Maxwells equations, including nonlinear terms resulting from the nonlinear dependence of the dielectric polarization on the applied field[28, 29]. From the view of photons as quantum mechanical particles, such an intensity-dependent refractive index can be reinterpreted in terms of binary interactions between photons. This picture of interacting photons was pioneered in the calculation of the effective third order nonlinear polarizability of the vacuum arising from the exchange of a virtual electron-positron pair[30, 31]. As an exciting perspective, topological photonics can be combined with optical nonlinearities, leading to new phenomena and novel strongly correlated states of light, such as an analog of the fractional quantum Hall effect. Thus bosons with controllable interaction is potential in a variety of platforms.

In terms of above consideration, we propose a bosonic hexagonal lattice model[26] with interactional bosons(Fig. 1) which are viewed as interactions between photons. The hexagonal lattice is an important two-dimensional lattice in condensed matter physics[25, 27] and it is crucial for of both experimental and theoretical reasons. Experimentally, the hexagonal lattice can be realized in graphene, which currently is a popular topic of research and an amazing material of fundamental importance and interest. Theoretically, the hexagonal lattice is also interesting because it has two sites per unit cell (A-sites and B-sites), so the model has to be a two-band model. As consideration below, we will give a new band structure which is different as before.

A. Model Hamiltonian

Consider an interactional bosonic hexagonal lattice model, with two different lattices A(B). In addition to general hexagonal lattice model, we need to add on-site bosonic interactions. Thus, we get the tight-binding

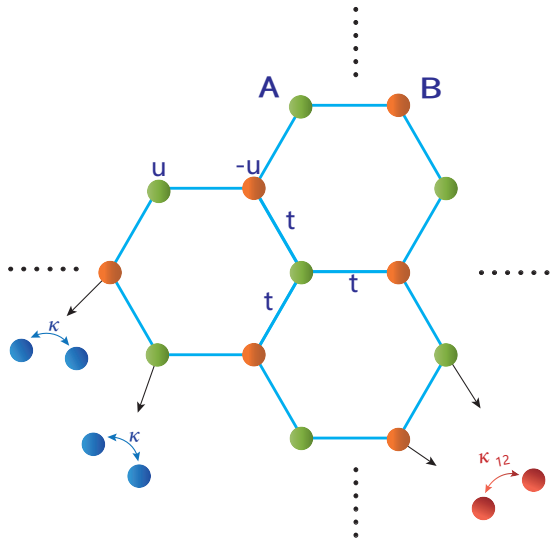

FIG. 1: Interactional bosonic hexagonal lattice model, where green(orange) spots represent lattice A(B), on-site potential energy for lattice A(B) is u(-u) and the interaction between two particles on the lattice A(B) is κ. Specially, κ_{12} denotes interaction on two bosons between lattice A and lattice B respectively.

Hamiltonian form,

$$\begin{aligned} H &= \sum_{l,m} u a^\dagger_{l,m} a_{l,m} - u b^\dagger_{l,m} b_{l,m} \\ &+ \sum_{l,m} t a^\dagger_{l,m} b_{l,m} + t a^\dagger_{l,m} b_{l-1,m} + t a^\dagger_{l,m} b_{l,m-1} + h.c. \\ &+ \sum_{l,m} \kappa/2 (a^\dagger_{l,m} a^\dagger_{l,m} a_{l,m} a_{l,m} + b^\dagger_{l,m} b^\dagger_{l,m} b_{l,m} b_{l,m}) \end{aligned} \tag{1}$$

where (l,m) represents the lattice site(l,m), which is the abbreviate from $\mathbf{r_{A(B)}}_{(l,m)} = l\mathbf{c_1} + m\mathbf{c_2}, \mathbf{r_A}_{(l,m)} = \mathbf{r_B}_{(l,m)} + \mathbf{c_0}$, where $\mathbf{c_1} = (1/2)[3, \sqrt{3}], \mathbf{c_2} = (1/2)[3, -\sqrt{3}]$ and $\mathbf{c_0} = [-1, 0]$. And $a(b)^\dagger_{l,m}(a(b)_{l,m})$ is the creation(annihilation) operator of bosons on the lattice site (l,m) for A(B), u is on-site potential, t is coupling strength between lattice A and lattice B, and κ is a nonlinear strength which is considered to be positive.

By virtue of Fourier transformation with consideration of periodical boundary condition(PBC), the stationary GP equation in the momentum space assumes the following form,

$$H(k_x, k_y)\psi(k_x, k_y) = E(k_x, k_y)\psi(k_x, k_y) \tag{2}$$

with

$$H(k_x, k_y) = \begin{pmatrix} d_z + \kappa|\psi_1(k_x, k_y)|^2 & d_x - id_y \\ d_x + id_y & -d_z + \kappa|\psi_2(k_x, k_y)|^2 \end{pmatrix} \tag{3}$$

where

$$\begin{aligned} d_x &= t\cos\mathbf{k}\cdot\mathbf{c_0} + t\cos\mathbf{k}\cdot\eta_\mathbf{1} + t\cos\mathbf{k}\cdot\eta_\mathbf{2} \\ d_y &= t\sin\mathbf{k}\cdot\mathbf{c_0} + t\sin\mathbf{k}\cdot\eta_\mathbf{1} + t\sin\mathbf{k}\cdot\eta_\mathbf{2} \\ d_z &= u \end{aligned} \tag{4}$$

with $\eta_\mathbf{1} = \mathbf{c_0} + \mathbf{c_1}$, $\eta_\mathbf{2} = \mathbf{c_0} + \mathbf{c_2}$, $\mathbf{k} = [k_x, k_y]$, and $k_x(k_y)$ is the quasimomentum along the $x(y)$ direction, and $\psi(k_x, k_y) = [\psi_1(k_x, k_y), \psi_2(k_x, k_y)]^T$ denotes a Bloch band state with two components.

In the following, all we need to do is to find energy band structure of this eigenstate dependent Hamiltonian. In the mean time, we will find the position where it gives more than two eigenvalue which are $\mathbf{k_1} = \frac{2\pi}{3}(1, \frac{1}{\sqrt{3}})$ and $\mathbf{k_2} = \frac{2\pi}{3}(1, -\frac{1}{\sqrt{3}})$, these two special points are called Nonlinear Dirac Points, and NDCs can be produced around them. And throughout this paper, we assume that all physical variables are in dimensionless unit.

B. Dynamical stability in the energy bands

We have already get the energy dispersion where there are four values above. However, we cannot know whether these eigenvalues are stable because of interactions. Thus we will consider the stability of eigenvalues[23]. Because we focus on the first two bands which can form the NDCs, we only give stability of these two values. For simplicity, we will focus on perturbations to the stationary solutions, and meanwhile we consider closed condition so that allowing us to use the time dependent GP equation in the momentum space. In order to analyze their time evolution, such perturbations can be generally written in pseudo-spinor components as

$$|\delta\psi(k_x, k_y, t)\rangle = \begin{pmatrix} \delta\psi_1(k_x, k_y, t) \\ \delta\psi_2(k_x, k_y, t) \end{pmatrix} \tag{5}$$

Consider now a stationary solution $|\psi(k_x, k_y, t)\rangle$ i satisfying eq in the above text with energy $E(k_x, k_y)$. Our aim is to evaluate the time evolution of a state initially prepared near such a stationary solution as given by$|\Psi(k_x, k_y, t)\rangle = |\psi(k_x, k_y, t)\rangle + |\delta\psi(k_x, k_y, t)\rangle$. If $|\Psi(k_x, k_y, t)\rangle$ does not go to infinity as $t \to \infty$, then the stationary solution is dynamically stable. For neater analysis, we may separate the dynamical phase from $|\Psi(k_x, k_y, t)\rangle$ as $|\Psi(k_x, k_y, t)\rangle = e^{-iEt}|\Phi(k_x, k_y, t)\rangle$, then we can get $|\psi(k_x, k_y, t)\rangle = e^{-iEt}|\psi(k_x, k_y, 0)\rangle$ and $|\delta\psi(k_x, k_y, t)\rangle = e^{-iEt}|\delta\phi(k_x, k_y, t)\rangle$. After some algebra, we can add its conjugate into the equation,

$$i\frac{\partial}{\partial t}\begin{pmatrix} \delta\phi_1 \\ \delta\phi_2 \\ \delta\phi_1^* \\ \delta\phi_2^* \end{pmatrix} = L\begin{pmatrix} \delta\phi_1 \\ \delta\phi_2 \\ \delta\phi_1^* \\ \delta\phi_2^* \end{pmatrix} \tag{6}$$

where

$$L = \begin{pmatrix} H_g + H_1 & H_2 \\ -H_2^* & -H_g^* - H_1 \end{pmatrix} \tag{7}$$

$$H_g = H(k_x, k_y, \psi(k_x, k_y, 0)) - E(k_x, k_y)I \tag{8}$$

$$H_1 = \kappa\begin{pmatrix} |\psi_1(k_x, k_y, 0)|^2 & 0 \\ 0 & |\psi_2(k_x, k_y, 0)|^2 \end{pmatrix} \tag{9}$$

$$H_2 = \kappa\begin{pmatrix} \psi_1^2(k_x, k_y, 0) & 0 \\ 0 & \psi_2^2(k_x, k_y, 0) \end{pmatrix} \tag{10}$$

We need to get the solution of $\psi(k_x, k_y)$ as the initial value and plug into equation above. Due to the resemblance of Eq with the time dependent Schrodinger equation in linear quantum mechanics, the time evolution of the perturbation is governed by the operator e^{-iLt}. However, since L is not a Hermitian operator, eigenvalues of L can in general be complex. It follows that in order for to be dynamically stable, all eigenvalues L_n of L must satisfy Im(L_n)=0, $\forall n$. Fig. 2 shows the maximum imaginary component of eigenvalues of L for the lowest two bands. It follows that the lowest energy band is dynamically stable throughout the BZ, while the second band is dynamically unstable.

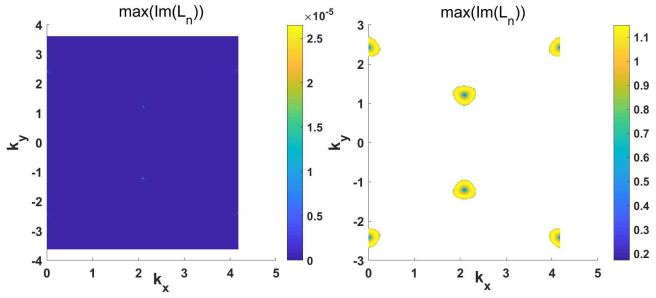

FIG. 2: max(Im(L_n)) for the lower two energy bands as a function of k_x and k_y.

C. NDCs in interactional bosonic hexagonal lattices

Fig. 3 shows the snapshots of the first two bands' structures. As expected from previous theoretical and experimental studies of nonlinear Bloch bands in zero- or one-dimensional systems, a self-crossing loop structure(NDC in 2D) emerges as κ increases beyond a critical value κ_c. Specifically, for $\kappa = \kappa_c$, the bottom band starts to produce a cone[in Fig. 3(c)]. For $\kappa > \kappa_c$, this structure appears. And meanwhile we find that the difference between linear and nonlinear model is that in the linear model we examine the Dirac points will close and reopen which correspond to energy gapless points and gapped points as parameters change, but in nonlinear model these points change features fundamentally which will be gapless points all the time once the parameters

reach critical value, not having the process of reopening the energy band, which will be useful for our calculations in Sec. III for Berry phase in nonlinear systems. Next, we examine the band structure for the whole 2D BZ, with special attention paid to the bottom band. In particular, subbands have grown from the bottom band(in Fig. 3(c)). Precisely at a Nonlinear Dirac Point of a looped subband, two of the four Bloch states are degenerate. Previously the Chern number of the lowest band distinguishes between topologically trivial and nontrivial phases in noninteracting Chern insulators in the linear counterpart($\kappa = 0$), if we still use this Chern number, though the lowest band is well separated from the upper band for $\kappa \leq \kappa_c$, we cannot define it due to the appearance of the self-crossing points which are touched each other in the first two bands for $\kappa > \kappa_c$. Now we need a new topological number to tell the difference based on κ. Thus it is necessary to consider a new topological invariant which is able to distinguish different topological phase in the lowest band.

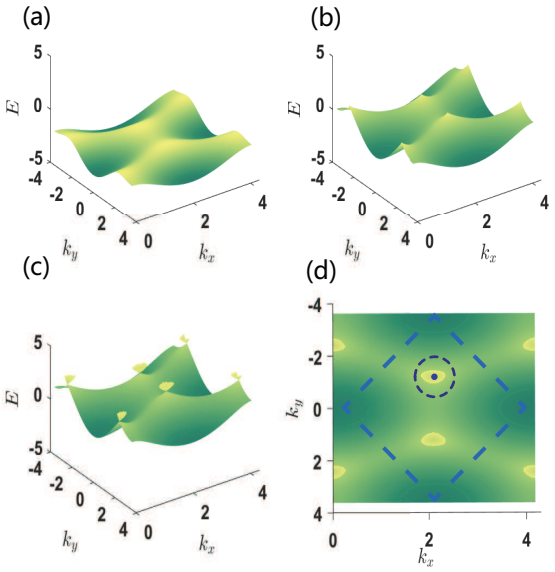

FIG. 3: The cone structure in interactional bosonic hexagonal lattice model, and here we only give dispersion relation of the first two energy band in order to be concise. The parameters chosen are $t = 1, u = 1.5, (a)\kappa = 0, (b)\kappa = 3, (c)\kappa = 5$. (d)Vertical view of (c), dashed lines denote Brillouin Zone(BZ), dashed circle denotes location of one of the nonlinear cones and point inside this circle denotes one of Nonlinear Dirac Points.

D. Effective Hamiltonian around Nonlinear Dirac Points

We make an approximation on Hamiltonian up to first order of $E = E^0 + E^1$, $d_i = d_i^0 + d_i^1, i = x, y, z$, where 0 and 1 represents zero-order and first-order respectively. Around Nonlinear Dirac Points $\mathbf{k_1} = \frac{2\pi}{3}\left(1, \frac{1}{\sqrt{3}}\right), \mathbf{k_2} = \frac{2\pi}{3}\left(1, -\frac{1}{\sqrt{3}}\right)$, we obtain the effective Hamiltonian,

$$H(k_x, k_y) = d_x^1\sigma_x + d_y^1\sigma_y - \frac{2uE^1}{\kappa}\sigma_z \tag{11}$$

where

$$\begin{aligned} d_x^1 &= -\frac{3\sqrt{3}}{4}t(k_x - \frac{2\pi}{3}) \mp \frac{3}{4}t(k_y \mp \frac{2\sqrt{3}\pi}{9}) \\ d_y^1 &= \frac{3}{4}t(k_x - \frac{2\pi}{3}) \mp \frac{3\sqrt{3}}{4}t(k_y \mp \frac{2\sqrt{3}\pi}{9}) \\ E^1 &= \pm\frac{\kappa\sqrt{(d_x^1)^2 + (d_y^1)^2}}{\sqrt{\kappa^2 - 4u^2}} \end{aligned} \tag{12}$$

That the two branches of the NDC are described by different effective Hamiltonians, which is because original Hamiltonian is related to the Bloch eigenstate.

III. NONLINEAR BERRY PHASE

A. Berry phase in nonlinear systems

Now we assume that the parameter vector is quasi-momentum $\mathbf{k}$ which varies slowly in time and then we give wave function $\psi(\mathbf{k}(t))$. In the meantime, we view Λ as the overall phase, which we take it to be phase of wave function $\psi(\mathbf{k}(t))$, $\Lambda = -arg(\psi(\mathbf{k_0}, t))$, where $\mathbf{k_0}$ is a fixed position in the momentum space so that we separate an overall phase from $\psi(\mathbf{k}(t))$, thus we can obtain $\psi(\mathbf{k}(t)) = e^{-i\Lambda}\phi(\mathbf{k}(t))$. We make approximation on $\phi(\mathbf{k}(t))$,

$$\phi(\mathbf{k}(t)) = \epsilon^0\phi^0(\mathbf{k}(t)) + \epsilon^1\phi^1(\mathbf{k}(t)) + \cdots \tag{13}$$

where we introduce the adiabatic parameter $\epsilon \sim \frac{d\mathbf{k}}{dt}$ which can be viewed as the measure of how slow the parameters change and ϵ^0, ϵ^1 denotes respectively zero-order and first-order of ϵ. $\phi^0(\mathbf{k}(t))$ and $\phi^1(\mathbf{k}(t))$ denotes zero-order and first-order of $\phi(\mathbf{k}(t))$. When the adiabatic parameter tends to zero, i.e., $\epsilon \to 0$, the adiabatic limit can be achieved. At last, we put the new formation of $\psi(\mathbf{k}(t))$ into time dependent Schrödinger equation. Consequently, the expression of the overall phase can be expanded in a perturbation series in the adiabatic parameter[32],

$$\frac{d\Lambda}{dt} = \Lambda_0(\epsilon^0) + \Lambda_1(\epsilon^1) + o(\epsilon^2) \tag{14}$$

In the quantum evolution with slowly changing parameters, $\phi^0(\mathbf{k}(t))$ is the wave function of the instantaneous eigenstate and $\phi^1(\mathbf{k})$ is induced by the system's slow change which also depends on the adiabatic parameter and is of order ϵ^1. Thus, we have the explicit expression,

$$\begin{aligned}&\Lambda_0(\epsilon^0) = E^0(\mathbf{k}(t))\\&\Lambda_1(\epsilon^1) = \sum_{\alpha=1,2} -i(\phi^0_\alpha)^*\frac{\partial}{\partial t}\phi^0_\alpha\\&+\kappa|\phi^0_\alpha|^2((\phi^0_\alpha)^*\phi^1_\alpha + \phi^0_\alpha(\phi^1_\alpha)^*)\end{aligned} \tag{15}$$

Where ϕ^0_α and ϕ^1_α represent pseudospin component of ϕ^0 and ϕ^1 respectively. Here we define $C_\alpha = (\phi^0_\alpha)^*\phi^1_\alpha + \phi^0_\alpha(\phi^1_\alpha)^*$, which can be obtained from equations below,

$$\sum_{\alpha=1,2} C_\alpha = 0 \tag{16}$$

$$\begin{aligned}&\sum_{\beta=1,2} g\phi^0_\alpha|\phi^0_\beta|^2 C_\beta - g\phi^0_\alpha C_\alpha\\&= \sum_{\beta=1,2} i(\phi^0_\alpha((\phi^0_\beta)^*\frac{\partial}{\partial t}\phi^0_\beta) - \frac{\partial}{\partial t}\phi^0_\alpha)\end{aligned} \tag{17}$$

The first one implies that $\phi^\dagger\phi = 1$, where $\phi = \phi^0 + \phi^1$, and then we set $(\phi^0)^\dagger\phi^0 = 1$ so that we obtain the value of $\sum_\alpha C_\alpha$. And the second one is obtained by putting $\phi = \phi^0 + \phi^1$ into nonliear Hamiltonian and then giving time dependent Schrödinger equation on ϕ^0. By virtue of above equations, we can get C_α.

When the quasimomentum move in a circuit, the eigenstate evolves for an infinitely long time duration in the adiabatic limit. The time integral of the zero-order term gives the so-called dynamic phase because it is closely related to the temporal process of the evolution. The time integral of the first-order term makes an additional contribution to the overall phase, which only depends on the geometry of the closed path in the parameter space. The higher-order terms vanish in the adiabatic limit $\epsilon \to 0$. Thus, we obtain Berry phase with the result of C_α in quasimomentum space.

B. Berry phase with effective Hamiltonian

Because of the appearance of NDCs in quasimomentum space, we use the effective Hamiltonian in Eq. (11) around Nonlinear Dirac Points regard to lower branch. First, we consider $\kappa < 2u$, and the eigenfunction,

$$\psi_-(t) = \begin{pmatrix}\phi^0_1\\ \phi^0_2\end{pmatrix} = \begin{pmatrix}\sin\frac{\theta}{2}\\ \cos\frac{\theta}{2}e^{i\varphi}\end{pmatrix} \tag{18}$$

with

$$\begin{aligned}&\tan\varphi(k_x,k_y) = \frac{d^1_y}{d^1_x}\\&\tan\theta(k_x,k_y)\\&= \frac{\sqrt{\kappa^2(\kappa-2u)^2 + 4E^1\kappa^2(\kappa-2u) + 4(E^1)^2(\kappa^2-4u^2)}}{4uE^1}\end{aligned} \tag{19}$$

where d^1_x and d^1_y are defined in Eq. (12), which is the same definition for $\kappa > 2u$. And form of E^1,

$$E^1 = \frac{D_0 - \sqrt{D_1((d^1_x)^2 + (d^1_y)^2) + D_2}}{F} \tag{20}$$

where we define,

$$\begin{aligned}D_0 &= 4u^3 - 4\kappa u^2 + 4\kappa^2 u\\D_1 &= 4(2u-\kappa)(10u-\kappa)u^2\\D_2 &= (2u-\kappa)^2(\kappa-2u)^2u^2\\F &= 20u^2 - 12\kappa u + \kappa^2\end{aligned} \tag{21}$$

By virtue of the form of Λ as well as the value of C_α in the last subsection,

$$\begin{aligned}\Lambda_1 &= \sum_{\alpha=1,2}\oint_D \frac{1}{2}\frac{\partial\varphi}{\partial\mathbf{k}}d\mathbf{k} + \oint_D i\cot\theta\frac{\partial\theta}{\partial\mathbf{k}}d\mathbf{k}\\&= 0\end{aligned} \tag{22}$$

where D represents a closed curve including Nonlinear Dirac Points. Though this curve include Nonlinear Dirac Points, they are not energy gapless points which can not result in singularity in this integral BZ. Thus, we obtain a zero Berry phase in this situation. Second, we consider $\kappa > 2u$ and obtain the same eigenfunction as in Eq. (18), but with different θ and φ,

$$\tan\varphi(k_x,k_y) = \frac{d^1_y}{d^1_x}, \quad \tan\theta = \frac{\sqrt{\kappa^2-4u^2}}{2u} \tag{23}$$

and Berry phase gives as follow,

$$\begin{aligned}\Lambda_1 &= \sum_\alpha -i\oint_D(\phi^0_\alpha)^*\frac{\partial}{\partial\mathbf{k}}\phi^0_\alpha d\mathbf{k} + \frac{1}{2}\oint_D(|\phi^0_1|^2 - |\phi^0_2|^2)\frac{\partial\varphi}{\partial\mathbf{k}}d\mathbf{k}\\&= \cos^2\frac{\theta}{2}2\pi + \frac{1}{2}(\sin^2\frac{\theta}{2} - \cos^2\frac{\theta}{2})2\pi\\&= \pi\end{aligned} \tag{24}$$

where D also represents a closed curve including Nonlinear Dirac Points, which are energy ungapped points at this time, leading to the nonzero Berry phase in nonlinear systems.

At last, we give a relation between Berry phase and the nonlinear strength κ

$$\Lambda_1 = \begin{cases}\pi, \kappa > 2u\\ 0, \kappa < 2u\end{cases} \tag{25}$$

where critical value of κ is $2u$.

C. Berry phase with eigenstate dependent Hamiltonian

We calculate Berry phase by virtue of effective Hamiltonian in the last subsection, which is concise to obtain results. Without generality, we will give a calculation based on eigenstate dependent Hamiltonian directly,

which is much more complex than calculation with effective Hamiltonian. However, it can provide a much more general prospective to consider Berry phase in nonlinear systems. First, we give the state dependent Hamiltonian,

$$H(\mathbf{k}) = d_x\sigma_x + d_y\sigma_y + d_z(E)\sigma_z \tag{26}$$

with

$$d_z(E) = u\Delta(E) \tag{27}$$

where we reduce state dependent Hamiltonian to energy dependent Hamiltonian and define,

$$\Delta(E) = \frac{2E(\mathbf{k}) - g}{2(E(\mathbf{k}) - g)} \tag{28}$$

and d_x, d_y are obtained in Eq. (4).

Similar to the last subsection, we can give an eigenfunction as the same before, but difference on form of θ and φ,

$$\tan\varphi(k_x, k_y) = \frac{d_y}{d_x}, \quad \tan\theta = -\frac{\sqrt{d_x^2 + d_y^2}}{d_z(E)} \tag{29}$$

Next, we do the same steps as before, considering $\kappa < 2u$ and $\kappa > 2u$ respectively. We construct any closed curve including Nonlinear Dirac Point $\mathbf{k_1}(\mathbf{k_2})$, which is only gapless under $\kappa > 2u$. In the meantime, we give the value of $E(\mathbf{k_1}(\mathbf{k_2}))$, which is $g - u$ when $\kappa < 2u$ and $g/2$ when $\kappa > 2u$. This imply that if $\kappa > 2u$, the area of this closed curve will appear a singularity localized on $\mathbf{k_1}(\mathbf{k_2})$ because the value of $E(\mathbf{k_1}(\mathbf{k_2}))$ make the denominator of integral function zero which we need to get complex connected closed curve to dig up this singularity and then calculate integral based on a small circle including singularity so that we can get nonzero Berry phase, however if $\kappa < 2u$, singularity will disappear in this area leading to the zero Berry phase. At last, we will get the same result in the last subsection.

IV. NUMERICAL RESULTS

A. Observable AB phase in nonlinear systems

More than 30 years ago, Berry delineated the effects of the geometric structure of Hilbert space on the adiabatic evolution of quantum mechanical systems[34]. These ideas have found widespread applications in physics and are routinely used to calculate the geometric phase shift acquired by a particle moving along a closed path so that a phase shift is determined only by the geometry of the path[33, 35] and is independent of the time spent enroute. Geometric phases provide an elegant description of the celebrated Aharonov-Bohm effect[36] where a magnetic flux in a confined region of space influences the eigenstates everywhere via the magnetic vector potential.

A recent study demonstrated the detection of a conventional 2D Dirac cone by use of an interference setup, similar in Fig. 4(a), where we consider phase difference between two time dependent state based on two evolution paths which we use the two semicircle paths for convenience in the following subsection including Nonlinear Dirac Points. This kind of setup will pave the way to full topological characterization of optical lattice systems. By virtue of this kind of setup, we can obtain the Berry phase associated with one nonlinear Dirac cone from direct numerical results based on the time-dependent GP equation, namely the adiabatic observable AB phase associated with two symmetric interfering paths which are showed in Fig. 4(a) enclosing the same nonlinear Dirac cone. The system parameters chosen are $t = 1, u = 1.5$. The two interfering paths in the momentum space to generate the observable AB phase are chosen as two small semicircles going around the NDCs, one clockwise and the other one counterclockwise. The system is forced to adiabatically move along the two paths which is similar to an AB effect experiment. The two interfering paths enclosing a nonlinear Dirac point are designed in the quasimomentum space, with the beam splitting and recombination executed adiabatically.

B. Fidelity in numerical simulation

First, we need to examine the difference between quasiadiabatic evolution state and instantaneous eigenstate in order that we can show phase shift numerically closed to our theoretical prediction if the quasiadiabatic evolution state tends to instantaneous eigenstate. For two symmetric semicircle paths in quasiadiabatic evolution process, we use the value of $d\phi/dt$ to approach the adiabatic state. Numerically, we can check whether this state is very close to the true adiabatical state, which is the instantaneous eigenstate of $H(t)$.

We define $|E(t)\rangle$ as the instantaneous eigenstate of $H(t)$. And then the fidelity of this system in the lowest energy state can be defined as $F(t) = |\langle E(t)|\psi(t)\rangle|^2$, where $|\psi(t)\rangle$ is the quasiadiabatic evolution state with small $d\phi/dt$. In order to achieve the aim of adiabatical state, we adjust the value of $d\phi/dt$ to achieve $F(t) \simeq 1$.

In the Fig. 4(b)and(c), we consider a complete evolution process where we can get a temporal fidelity which is defined as two states difference between instantaneous eigenstate and quasiadiabatic evolution state, and we examine that fidelity is almost one in the whole process, which we conclude that the quasiadiabatic evolution state is close to instantaneous eigenstate so that we can obtain observable AB phase numerically. At last, we can view the quasiadiabatic evolution state as the adiabatic state.

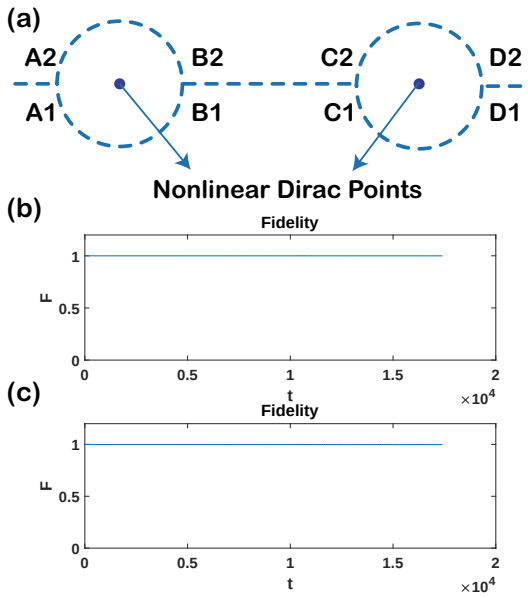

FIG. 4: (a)The two symmetry complete paths $A1-B1-C1-D1$ and $A2-B2-C2-D2$. (b) and (c) are fidelity of these two symmetry complete paths in the adiabatic evolution respectively. The value of $d\phi/dt$ we choose is 10^{-3}.

C. Numerical simulation of adiabatic evolution

Consider this interference approach: Two interfering paths share the same starting point and both go around Nonlinear Dirac Points in a symmetric manner, with one clockwise and the other one counterclockwise. In the $\kappa > \kappa_c$ regime with all other system parameters fixed, the parameter given in is a constant along each path. After the system has been forced to adiabatically travel along the two respective paths, we look into their phase difference, called the observable AB phase here.

Explicit implementations of how the initial state is split and recombined, as well as how quasimomenta k_x and k_y are adiabatically varied, are needed in the following part below. And we will give a simple explanation. We first solve Eq. (3) at initial position numerically and find energy dependent stationary solution for the lowest energy dispersion. This state is chosen as the initial condition and then evolved adiabatically following clockwise or counterclockwise semicircle with a radius $R = 10^{-4}$ in the momentum space, as sketched in the Fig. 4(a). The full circle is chosen as $k_x(t) = k_{x_0} + R\cos\phi(t)$ and $k_y(t) = k_{y_0} + R\sin\phi(t)$, where k_{x_0}, k_{y_0} represents position of Nonlinear Dirac Points, with $\phi(t)$ being the slowly varying parameter in time t as $d\phi/dt$ is defined in the last subsection. Numerically, the actual time evolution states are obtained by use of ordinary different equation numerical method.

Here we analyze two simulations: one is adiabatically travelling paths enclosing one of NDCs as $A1-B1$ path and $A2-B2$ path depict in Fig. 4(a). And the other is adiabatically travelling paths enclosing all NDCs in BZ as $A1-B1-C1-D1$ path and $A2-B2-C2-D2$ path in Fig. 4(a). In our simulation, we choose the total time of adiabatic evolution $T = 2\pi * 10^3$ in the first simulation and $T = 4\pi * 10^3 + (\mathbf{k_{y02}} - \mathbf{k_{y01}} + 2R)/f$ where f is the variance rate in $B1-C1$ and $B2-C2$ in the second simulation, and meanwhile we choose number of time intervals $N = 10^6$ so as to achieve a nearly adiabatic evolution and a higher numerical precision. And then we give $dt = T/N$ is a succulently small time interval. Finally, the evolution ends at $(k_x, k_y) = (k_x(T), k_y(T))$, where the phase difference of the two states accumulated following the two symmetric paths is found in the phase difference between these two states.

The first simulation implies that the adiabatic observable AB phase is quantized in π. As depict in Fig. 4(a), the observable AB phase is zero in the absence of nonlinear Dirac cones. When $\kappa > \kappa_c$, the adiabatic observable AB phase changes discontinuously to π. Thus the adiabatic observable AB phase is actually quantized in π. For the results shown in Fig., the two paths enclosing an NDC are chosen to be two small semicircles. We have considered other path geometries and the same results are obtained. The experimentally measurable AB phase obtained here is thus smoking-gun evidence of the formation of an NDC. Thus this is the same as Berry phase we discussed theoretically.

In the second simulation, we can set two new symmetric paths which include all nonlinear cones in BZ. In our case, we have two cones in BZ and we can set the paths like in Fig. 4(a). Now we calculate the phase difference of the two states which is related to time t. And then we observe the difference in phase while the evolution time t is increasing. For $\kappa > \kappa_c$, At the beginning

In the Fig. 5, we give a phase difference between two adiabatic evolution states temporally in the $\kappa > 2u$ regime where gapless points appear. First, these two states are set initially in start point $A1$ and $A2$ where they don't have phase difference in initial paths which is showed in area A. Next, these two states arrive at $B1$ and $B2$ and then travel along $B1-C1$ and $B2-C2$, at this time phase difference is π in $B1-C1$ and $B2-C2$, which is denoted in area B. At last, the two states travel along two complete paths and phase difference is back to zero, which is depicted in area C.

V. OTHER SITUATIONS

In this section, we will analyze some interesting results based on our hexagonal lattice model with some extra additions. First, we consider how additional term κ_{12} influence observable AB phase, and then we study robustness of these NDCs by adding some perturbations in Hamiltonian. At last, we add some noise randomly in the evolution paths to simulate realistic situations experimentally.

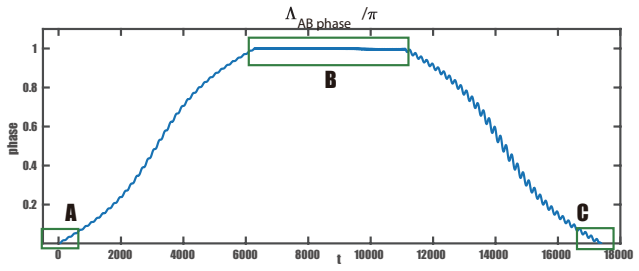

FIG. 5: Phase difference between two adiabatic evolution state in two symmetry complete paths around Nonlinear Dirac Points vs time t, and we examine three green squares represent appearance of phase 0 and phase π respectively. All parameters are fixed as the same as before, specially $\kappa = 5$ and $f = -0.5 * 10^{-3}$.

A. Additional interaction term κ_{12}

There are many kinds of bosonic interaction to consider in our hexagonal lattice. Interestingly, we examine that bosonic interactions on two different lattice A and B can control observable AB phase directly, as depicted in Fig. 1. Because of this, we can introduce an additional interactional term κ_{12} to achieve this process, and meanwhile we can give a new Hamiltonian including κ_{12} in Eq. (1),

$$\begin{aligned} H &= \sum_{l,m} u a^{\dagger}_{l,m} a_{l,m} - u b^{\dagger}_{l,m} b_{l,m} \\ &+ \sum_{l,m} t a^{\dagger}_{l,m} b_{l,m} + t a^{\dagger}_{l,m} b_{l-1,m} + t a^{\dagger}_{l,m} b_{l,m-1} + h.c. \\ &+ \sum_{l,m} \kappa/2 (a^{\dagger}_{l,m} a^{\dagger}_{l,m} a_{l,m} a_{l,m} + b^{\dagger}_{l,m} b^{\dagger}_{l,m} b_{l,m} b_{l,m}) \\ &+ \sum_{l,m} \kappa_{12} a^{\dagger}_{l,m} b^{\dagger}_{l,m} b_{l,m} a_{l,m} \end{aligned} \tag{30}$$

As the same we do in Eq. (1), we need to give an effective Hamiltonian with Eq. (30) and then we can obtain E^1,

$$E^1 = \pm \frac{\kappa(\kappa - \kappa_{12})\sqrt{(d^1_x)^2 + (d^1_y)^2}}{\sqrt{(\kappa - \kappa_{12})^2 - 4u^2}} \tag{31}$$

Referring to the previous discussion, we can give the $\kappa_c = \kappa_{12} + 2u$ where κ_{12} is viewed as an extra constant in this value. If we make an observation on AB phase numerically, the critical line κ_c moves at the value of κ_{12}.

B. Robustness of NDCs

In the noninteractional Chern insulator, Dirac cones will disappear with the mass term. In contrast to the Chern insulator, we want to know whether these NDCs are detroyed by a mass term like the Chern insulators.

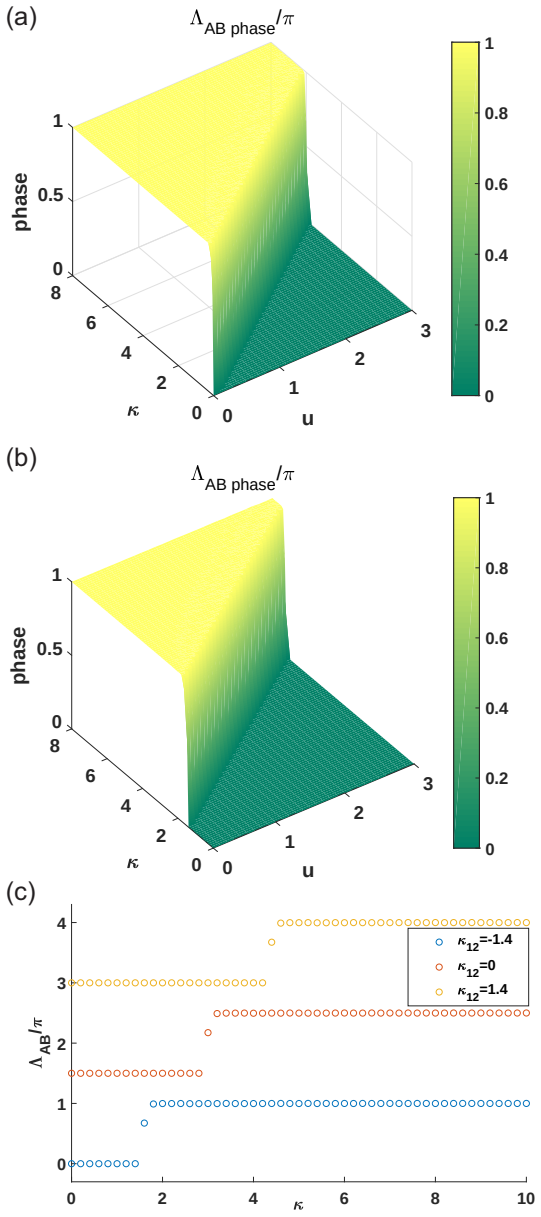

FIG. 6: (a)and(b) denote observable AB phase vs u and κ in the interactional bosonic hexagonal lattice model with or without an additional interactional term $\kappa_{12} = 1.5$, and we can see the moving of critical line $\kappa_c = \kappa_{12} + 2u$. (c)When $u = 1.5$ and $\kappa_{12} = -1.4, 0, 1.4$, observable AB phase vs κ, which are offset vertically for clarity. Specially, $\kappa_{12} = 0$ denotes that we are back to the situation where we only consider interactional term with κ.

If we introduce a perturbation term which is small $H_p = g_x\sigma_x + g_y\sigma_y + g_z\sigma_z$ into the Hamiltonian Eq. (3), we find that these NDCs are robust to perturbations. The Nonlinear Dirac Points in our system will be changed by this small perturbation. And then we get these points

k_1', k_2' and effective Hamiltonian,

$$H_{effc} = (d_x^1 + g_x)\sigma_x + (d_y^1 + g_y)\sigma_y - \frac{2(u+g_z)E^1}{\kappa}\sigma_z \tag{32}$$

where

$$E^1 = \pm\kappa\sqrt{\frac{(d_x^1+g_x)^2 + (d_y^1+g_y)^2}{\kappa^2 - 4(u+g_z)^2}} \tag{33}$$

whose values are given in II D, and g_x, g_y and g_z are perturbations.

In the Fig. 7, we examine that Nonlinear Dirac Points are on the original poistion while this position varies a little when we set $g_x = 0.35$, $g_y = 0.3$ and $g_z = 0.22$.

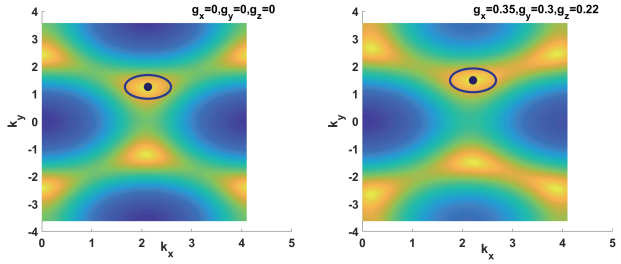

FIG. 7: Robustness of nonlinear cones with perturbation and its value we choose is arbitrary whose perturbation is small enough.

C. Random noise in the evolution

Experimentally, we make these two evolution paths with interference set up, which can be influenced by random pertubations in these paths indispensably. Next, if we consider these two paths which are perturbed by random noise temporally. In order to check whether Berry phase is discount numerically, we still consider the observable AB phase, this time we need to add some random noise to the two symmetric paths. Importantly, we can make a comparison between the observable AB phase above with and without random noise. Now we introduce a random Hamiltonian $H_{random}(t) = \mathbf{d}_{random} \cdot \sigma$, which is sufficiently small in order to simulate random noise in real evolution process which is not very large. And then we get the result from Fig. 8, which implies that discount Berry phase is not quantized even if we add small random noise.

VI. DISCUSSION

It is interesting to discuss the system parameters u and κ, then we obtain phase vs system parameters u and κ in Fig. 6(a). In the noninteracting Chern insulator model,

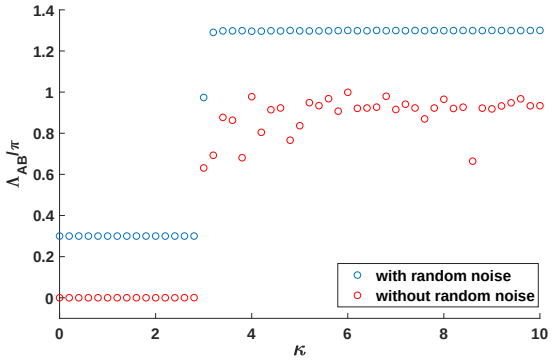

FIG. 8: The observable AB phase is changeable when we add random noise temporally, which are offset vertically for clarity, and strength of this random noise we consider is $1.5 * 10^{-4}$. Other parameters are the same as before.

u can be the massive term to break down the symmetry, and various u also represents open and closed in band gap. This behavior is observed in the interacting case with $\kappa > \kappa_c$, though Nonliear Dirac Points will be closed all the time if it starts to close from $\kappa = \kappa_c$. Interestingly, with the emergence of NDCs ($\kappa > \kappa_c$), their Berry phase stays to be unity and the observable adiabatic AB phase remains quantized in π numerically. In particular, phases with different value of u which are symbols of noninteracting topological transition could have the same value of Berry phase and hence they can be categorized into the same topological phase depicted in Fig. 6. This clearly shows the possibility of two topologically distinct phases to become topologically equivalent result from interaction, and meanwhile we find that Nonlinear Dirac Points are different from Dirac Points in the linear systems where they can close and reopen the energy bands, however Nonlinear Dirac Points only have the process of closing, not reopening the energy bands. In the following, we make some discussions on hexagonal lattice with interactions on different lattice, robustness of NDCs and random noise effect in quasievolution.

VII. CONCLUSION

In conclusion, we have discovered an interaction induced quantum phase transition featured by NDCs. The NDCs will appear when the parameter $\kappa > \kappa_c$, and meawhile they are robust against small perturbations. In addition, they have special pseudospin structures, remarkable band structures, and quantized Berry phases in effective Hamiltonian and state dependent Hamiltonian. Given a observable adiabatic AB phase numerically, we show that it is still quantized in π which is associated with Berry phase theoretically. And interestingly, we can adjust κ_{12} to move the critical value κ_c so that we are able to control appearance of NDCs. In the meantime, we think Berry phase in interactional systems can be a

directly topological number to analyze lattice model with bosonic interactions.

Note added: When we finished this Manuscript, we had noticed that in a recent paper, $arXiv$: 2006.09753, the authors developed a method to obtain a general expression for nonlinear Zak phases and discuss the topological phase induced by the nonlinearity in real and momentum space.

[1] Xiao, Di, M. C. Chang, and Q. Niu, Berry phase effects on electronic properties, Rev. Mod. Phys. **82**, 1959(2010).

[2] D.J.Thouless, et al, Quantized Hall Conductance in a Two-Dimensional Periodic Potential, Phys. Rev. Lett. **49**, 405.

[3] M.Kohmoto, B.I.Halperin, and Y.S.Wu, Diophantine equation for the three-dimensional quantum Hall effect, Phys. Rev. B **45**, 13488.

[4] D.J.Thouless, Quantization of particle transport, Phys. Rev. B **27**, 6083.

[5] H.Xue, Y.Yang, F.Gao, et al, Acoustic higher-order topological insulator on a kagome lattice, Nat. Mater. **18**, 108(2019).

[6] Y.L.Chen, J.G.Analytis, J.H.Chu, et al, Experimental Realization of a Three-Dimensional Topological Insulator, Bi2Te3, Science. **325**, 5937(2009).

[7] X.L.Qi, and S.C.Zhang, Topological insulators and superconductors, Rev. Mod. Phys. **83**, 1057(2010).

[8] Bernevig, B, Andrei, et al. Quantum Spin Hall Effect and Topological Phase Transition in HgTe Quantum Wells, Science **314**, 5806(2006).

[9] S.Ryu, A.P.Schnyder, A.Furusaki, et al, Topological insulators and superconductors: tenfold way and dimensional hierarchy, New Journal of Physics. **12**(6):065010.

[10] W.Pook, and J.Hajdu, On the topological explanation of the integer quantum hall effect, Zeitschrift Fr Physik B Condensed Matter. **66**, 427(1987).

[11] Simon, and Barry, Holonomy, the Quantum Adiabatic Theorem, and Berry's Phase, Phys. Rev. L. **51**, 2167(1983).

[12] Y.Hadad, A.B.Khanikaev, Al, and Andrea, Self-induced topological transitions and edge states supported by nonlinear staggered potentials, Phys. Rev. B **93**, 155112(2016).

[13] Y.V.Kartashov, and D.V.Skryabin, Bistable Topological Insulator with Exciton-Polaritons, Phys. Rev. L. **119**, 253904(2017).

[14] Yonatan, Sharabi, Hanan, et al, Self-Induced Diffusion in Disordered Nonlinear Photonic Media, Phys. Rev. L. **121**, 233901(2018).

[15] D.Leykam, and Y.D.Chong, Edge Solitons in Nonlinear-Photonic Topological Insulators, Phys. Rev. L. **117**, 143901(2016).

[16] L.Fidkowski, and A.Kitaev, Effects of interactions on the topological classification of free fermion systems, Phys. Rev. B **81**(13):134509(2009).

[17] C.Wang, A.C.Potter, and T.Senthil, Classification of Interacting Electronic Topological Insulators in Three Dimensions, Science **343**, 6171(2014).

[18] X.Y.Song, and A.P.Schnyder, Interaction effects on the classification of crystalline topological insulators and superconductors, Phys. Rev. B **95**, 195108(2017).

[19] Leggett, J.Anthony, Bose-Einstein condensation in the alkali gases: Some fundamental concepts, Rev. Mod. Phys. **73**, 307(2001).

[20] F.Dalfovo, S.Giorgini, L.P.Pitaevskii, et al, Theory of Bose-Einstein condensation in trapped gases, Rev. Mod. Phys. **71**, 463(1999).

[21] J.Liu, B.Wu, and Q.Niu, Nonlinear Evolution of Quantum States in the Adiabatic Regime, Phys. Rev. L. **90**, 170404(2003).

[22] J.Liu, L.B.Fu, B.Y.Ou, et al, Theory of nonlinear Landau-Zener tunneling, Phys. Rev. A **66**, 207(2001).

[23] R.W.Bomantara, W.Zhao, L.Zhou, et al. Nonlinear Dirac cones, Phys. Review. B **96**, 121406(2017).

[24] Tomoki Ozawa, Hannah M. Price, Alberto Amo, Nathan Goldman, Mohammad Hafezi, Ling Lu, Mikael C. Rechtsman, David Schuster, Jonathan Simon, Oded Zilberberg, and Iacopo Carusotto Rev. Mod. Phys. **91**, 015006

[25] C.L.Kane, et al, Quantum Spin Hall Effect in Graphene, Phys. Rev. L. **95**, 226801(2005).

[26] Bernevig, and Hughes, Topological Insulators and Topological Superconductors(2013)

[27] F.D.M.Haldane, Model for a Quantum Hall Effect without Landau Levels: Condensed-Matter Realization of the "Parity Anomaly", Phys. Rev. L. **61**, 2015(1988).

[28] A.Lakhtakia, and T.G.Mackay, Negative refraction by quantum vacuum, physics(2007).

[29] R.Karplus, The Scattering of Light by Light, Phys. Rev. **83**, 776(1951).

[30] R.W.Boyd, and B.R.Masters, Nonlinear Optics, Third Edition, Journal of Biomedical Optics. **14**,029902(2009).

[31] P.N.Butcher, and D.Cotter, The Elements of Nonlinear Optics Symmetry properties, 10.1017/CBO9781139167994(5):122-149(1990).

[32] J.Liu, and L.B.Fu, Berry phase in nonlinear systems, Phys. Rev. A **81**, 052112(2010).

[33] L.Duca, T.Li, M.Reitter, et al, An Aharonov-Bohm interferometer for determining Bloch band topology, Science. **347**, 6219(2015).

[34] M.V.Berry, Quantal Phase Factors Accompanying Adiabatic Changes, Proceedings of the Royal Society A Mathematical, 1984.

[35] F.Wilczek, and A. Shapere, Advanced Series in Mathematical Physics, Geometric Phases in Physics Volume **5**, SOME APPLICATIONS AND TESTS, 0613(1989).

[36] Y.Aharonov, and D. Bohm, Significance of Electromagnetic Potentials in the Quantum Theory, Phys. Rev. **115**, 485(1959).